

C-SNAP: Coupled
SACLANTCEN normal
mode propagation loss model

C.M. Ferla, M.B. Porter and F.B. Jensen

The content of this document pertains to work performed under Project 19 of the SACLANTCEN Programme of Work. The document has been approved for release by The Director, SACLANTCEN.

Issued by:
Underwater Research Division

W.I. Roderick
Division Chief

**C-SNAP: Coupled SACLANTCEN
normal mode propagation loss model**

C.M. Ferla, M.B. Porter and F.B. Jensen

Executive Summary: In ocean environments where either the water depth, the sound-speed profile, or the bottom composition vary significantly over the propagation path, sonar performance predictions cannot be satisfactorily addressed without taking into account the range-dependent properties of the environment. Though several numerical models are currently available for solving propagation problems in range-dependent environments, they tend to be quite sophisticated and their correct use requires considerable skill on the part of the model user. This report describes a coupled-mode range-dependent model built with the main objective of being particularly easy to handle and competitive in terms of execution time with the existing parabolic equation algorithms. The code, which is written in standard Fortran, is highly portable and can be easily implemented on a personal computer.

Our approach consists in generalizing the range-independent problem to a range-dependent one by dividing the propagation path in a sequence of range-independent segments and using normal modes to represent the acoustic field in each segment. We take advantage of a widely used finite-difference algorithm for solving the range-independent problem and make the assumption that the acoustic field is dominated by the outgoing component. The code incorporates a reliable algorithm for the automatic selection of the vertical grid spacing to be used for accurately marching the solution out in range. We also bypass the calculation of mode coupling matrices and compute the mode coefficients in a new segment by projecting the pressure field onto the new mode set. To preserve accuracy, an energy-conserving matching condition is implemented at the coupling interfaces.

Limitations and areas of possible improvement are outlined.

**C-SNAP: Coupled SACLANTCEN
normal mode propagation loss model**

C.M. Ferla, M.B. Porter and F.B. Jensen

Abstract: On the basis of a widely used and efficient range-independent normal mode code, SNAP, and a numerical solution technique for one-way mode coupling obtained from KRAKEN, we have built a range-dependent propagation loss model called C-SNAP. While the mathematical aspects of the problem have already been described in detail, here we present the implementation of the model and give a detailed discussion of the numerical considerations that are fundamental to its accurate and efficient use. Finally the use of the model is illustrated by a series of examples.

Keywords: coupled modes ◦ energy conservation ◦ normal modes ◦ numerical modelling ◦ propagation loss ◦ range dependence

Contents

1. Introduction	1
2. Program overview	2
2.1. <i>The mathematical model</i>	2
2.2. <i>The environmental model</i>	5
2.3. <i>The program structure</i>	5
3. Installation of C-SNAP	7
4. Running C-SNAP	8
4.1. <i>Input structure</i>	8
4.2. <i>Environmental inputs</i>	9
4.3. <i>Changing default parameters</i>	12
4.4. <i>Computational inputs</i>	12
4.5. <i>Numerical considerations</i>	13
5. Examples	15
5.1. <i>Case 1 – Upslope propagation in a wedge-shaped waveguide</i>	15
5.2. <i>Case 2 – Downslope propagation in a wedge-shaped waveguide</i>	16
5.3. <i>Case 3 – Deep water propagation over a seamount</i>	17
5.4. <i>Numerical parameters and CPU times for cases 1, 2 and 3</i>	17
6. Conclusions	19
References	20
Appendix A – Graphical illustration of the geometry for the three test cases and comparison of the results	21
Appendix B – Program structure, command files, and input runstreams for the three test cases	29
Appendix C – Summary of C-SNAP inputs	37

1

Introduction

Despite the great achievements obtained with fast field and parabolic equation models, normal mode programs still remain a very efficient, simple, and practical tool for describing ocean acoustics in range-independent environments. In particular, various algorithms have been devised for normal mode codes to relieve the user from the task of ensuring the stability of the answer, a property which is usually dependent on the choice of model parameters not strictly related to the formulation of the physical problem.

Consequently, further to the development of an efficient numerical solution for normal mode coupling (KRAKEN [2]), we have built this range-dependent coupled mode model, C-SNAP, with the objective of maintaining many of the features which make the range-independent version so attractive and still compare favourably with other models in terms of speed and accuracy for a number of problems.

The SACLANTCEN range-independent normal mode program SNAP [1] was taken as the main building block on top of which range-dependent features have been added. While restructuring the code architecture some attention has been given to make the code suitable also for parallel processing.

2

Program overview

2.1. THE MATHEMATICAL MODEL

For ocean acoustic problems in a range-independent environment, the normal mode representation of the acoustic pressure produced by a harmonic point source in a horizontally stratified medium is given by the following expression:

$$p(r, z) = \frac{i}{4\rho(z_s)} \sum_{m=1}^{\infty} \Psi_m(z_s) \Psi_m(z) H_0^1(k_m r), \quad (1)$$

where r is the range, z the depth, ρ the density, z_s the source depth, Ψ_m the mode amplitude, H_0^1 the zero-order Hankel function of the first kind, k_m is the eigenvalue, and we have chosen to limit the solution to the outgoing travelling wave as ocean acoustic problems are often dominated by this component only (one-way propagation).

In our implementation of the above equation we use the large-argument asymptotic approximation of the Hankel function and neglect the contribution of the continuous spectrum. With M indicating the largest-order discrete mode of the problem, we come to the following final expression:

$$p(r, z) = \frac{i}{\rho(z_s) \sqrt{8\pi r}} e^{-i\pi/4} \sum_{m=1}^M \Psi_m(z_s) \Psi_m(z) \frac{e^{ik_m r}}{\sqrt{k_m}}. \quad (2)$$

The numerical method employed to find the mode amplitudes is based on a widely used finite-difference algorithm in combination with an inverse iteration technique. The eigenvalues of the problem may be successively refined over a sequence of meshes and finally extrapolated to yield the solution of an infinitely dense mesh, thus resulting as an improved estimate of the solution of the continuous problem [4].

Loss mechanisms such as volume attenuation in the water column, bottom absorption, shear, and scattering from surface and bottom boundaries are included in the imaginary part of the eigenvalue k_m . They are computed through a perturbational approach.

We define transmission loss in dB re 1 m as

$$\text{TL}(r, z) = -20 \log \left| \frac{p(r, z)}{p_0(r=1)} \right| \quad (3)$$

with

$$p_0(r) = e^{ik_0 r} / 4\pi r \quad (4)$$

being the pressure for the source in free space. The resulting expression for coherent transmission loss is

$$\text{TL}^{\text{coh}}(r, z) = -20 \log \left[\frac{1}{\rho(z_s)} \sqrt{\frac{2\pi}{r}} \left| \sum_{m=1}^M \Psi_m(z_s) \Psi_m(z) \frac{e^{ik_m r}}{\sqrt{k_m}} \right| \right]. \quad (5)$$

Similarly, by summing up the modes with a uniformly distributed random phase, we obtain the incoherent representation of the transmission loss:

$$\text{TL}^{\text{inc}}(r, z) = -20 \log \left[\frac{1}{\rho(z_s)} \sqrt{\frac{2\pi}{r}} \sqrt{\sum_{m=1}^M \left| \frac{\Psi_m(z_s) \Psi_m(z) e^{ik_m r}}{\sqrt{k_m}} \right|^2} \right]. \quad (6)$$

This quantity is particularly useful whenever the detailed interference structure presented by the coherent summation of modes is not physically meaningful and a smoothed result is preferred.

The range-dependent case is solved by generalizing the one-way formulation of the range-independent solution as follows:

- (a) Subdividing the propagation path in a sequence of range-independent segments, with sloping bottoms treated by the staircase approximation. Environmental properties for the various range subdivisions are obtained through a linear interpolation in range between adjacent profile inputs.
- (b) Finding the normal modes, the eigenvalues and the associated properties in the first segment and computing the pressure field as in the range-independent case until the interface to the next segment is reached.
- (c) The mode set pertaining to the next segment is computed and the pressure field to the left of the interface is projected onto the new mode set. The resulting mode coefficients (excitation coefficients) are then used to carry on the computation of the pressure field in the new segment. This procedure is repeated for each new segment.

As suggested by Evans [5], we formulate the general solution for the pressure field in the j th segment with ratios of Hankel functions as

$$p^j(r, z) = \sum_{m=1}^{M^j} a_m^j \frac{H_0^1(k_m^j r)}{H_0^1(k_m^j r_{j-1})} \Psi_m^j(z), \quad (7)$$

where r_{j-1} is the range at the j th interface, $r_{j-1} \leq r \leq r_j$, and in the first segment ($j = 1$) as a special case we set $r_j - 1 = r_1$ and define the mode coefficients as

$$a_m^1 = \frac{i}{4\rho(z_s)} \Psi_m^1(z_s) H_0^1(k_m^1 r_1). \quad (8)$$

Also, to preserve accuracy we use the interface condition suggested by Collins and Westwood [6] and implemented in a PE code [7]. This approach, which we will refer to as an impedance matching technique, consists in matching $p/(\rho c)^{1/2}$ across each interface.

By observing that at the beginning of each interface the ratio of the Hankel functions is always equal to one, we write the condition of continuity of pressure at the j th interface as

$$\frac{1}{\sqrt{\rho_{j+1}(z)c_{j+1}(z)}} \sum_{m=1}^{M^{j+1}} a_m^{j+1} \Psi_m^{j+1}(z) = \frac{1}{\sqrt{\rho_j(z)c_j(z)}} \sum_{m=1}^{M^j} a_m^j \frac{H_0^1(k_m^j r)}{H_0^1(k_m^j r_{j-1})} \Psi_m^j(z). \quad (9)$$

If we now apply to Eq. (9) the operator

$$\int (\cdot) \frac{\Psi_l^{j+1}(z)}{\sqrt{\rho_{j+1}(z)}} dz \quad (10)$$

and take advantage of the orthogonality property of the modes,

$$\int \frac{\Psi_l(z)\Psi_m(z)}{\rho(z)} dz = \delta_{lm}, \quad l, m = 1, \dots, M, \quad (11)$$

we obtain the a_l^{j+1} terms (excitation coefficients) as

$$a_l^{j+1} = \int \sum_{m=1}^{M^j} a_m^j \frac{H_0^1(k_m^j r)}{H_0^1(k_m^j r_{j-1})} \frac{\Psi_m^j(z)\Psi_l^{j+1}(z)}{\sqrt{\rho_j(z)\rho_{j+1}(z)c_j(z)/c_{j+1}(z)}} dz, \quad l = 1, \dots, M^{j+1}, \quad (12)$$

or equivalently, by properly grouping the terms as in Eq. (7),

$$a_l^{j+1} = \int p^j(r_j, z) \frac{\Psi_l^{j+1}(z)}{\sqrt{\rho_j(z)\rho_{j+1}(z)c_j(z)/c_{j+1}(z)}} dz, \quad l = 1, \dots, M^{j+1}. \quad (13)$$

The above is the actual expression evaluated at each interface by C-SNAP. It only requires the pressure field over depth to the left of the interface and the eigenfunctions in the new range segment.

In the actual implementation of the code we replace the Hankel functions with their large-argument asymptotic representation. Other interface conditions such as pressure matching and reduced-pressure matching [8] are also obtainable from C-SNAP and may be convenient in comparing results with different models.

2.2. THE ENVIRONMENTAL MODEL

As shown in Fig. A1 in Appendix A, the different segments used to describe the range-dependent environment are treated as a half-space subdivided into three main layers consisting of a water column of depth H_0 , a sediment layer of thickness H_1 , and a semi-infinite homogeneous subbottom. The sound speeds c_0 in the water column and c_1 in the sediment layer may vary with depth, while density (ρ_0, ρ_1) and volume attenuation (β_0, β_1) are kept constant within the two layers. The subbottom is treated as a solid with depth independent properties: c_2 is the compressional speed, ρ_2 the density, β_2 the compressional attenuation, c_{2s} is the shear speed and β_{2s} the shear attenuation. Furthermore, the sea surface and the seafloor are treated as rough boundaries, with s_0 and s_1 indicating the rms wave height.

The environment between any two input profiles is approximated by a series of range-independent segments with a sloping bottom being described by a staircase approximation. In Fig. A2 we show a case with distinct slopes at both the water-sediment and sediment-subbottom interfaces. The symbols P_1, P_2 , and P_m denote the location of the different input profiles used to represent the range-dependent environment, S_1, S_2 , and S_n are the range-independent segments used for representing a sloping bottom via a staircase approximation, r_1, r_2 , and r_n are the positions of the interfaces between adjacent segments where the mode coupling is performed. The number of range subdivisions between any consecutive input profiles (P_j, P_{j+1}) is controlled by an input parameter. The environmental properties in each of the resulting segments are obtained through linear interpolation in range.

In the case of a sloping bottom, the interpolation to compute the sound-velocity profile in the water and/or in the sediment layer is performed after the shallowest sound-velocity profile is extended with data points from the deepest one. Also, these data points are adjusted through a parallel shift in order to match the last point in the shallowest sound-velocity profile. Care should be taken to ensure that this technique is adequate to describe the expected environment.

2.3. THE PROGRAM STRUCTURE

A positive consequence of restricting the solution of the wave equation to the outgoing travelling component only is that this approach leads to equations which can be solved simply by marching forward in range. Furthermore, by replacing a true mode coupling calculation with that of the excitation coefficients, only the pressure field to the left of the interface and the mode set for the segment to the right of the interface are required at any time, with a substantial saving in terms of both storage and CPU time. However, while the computational output is usually required over a relatively sparse grid in depth, both the mode sets and the pressure fields over depth must be tabulated on very fine grids in order to preserve accuracy in the coupling process. The result is that huge amounts of data need to be handled when the environment has to be approximated by thousands of segments, with hundreds of modes in each segment. To solve this problem while keeping the program size

to a manageable level and minimizing the influence of I/O performance, we have chosen to arrange the program structure so that at the interface between two segments we compute simultaneously, on a mode-by-mode basis, both the excitation coefficients and the pressure field over depth at the end of the new segment. The result of combining these features is shown by the flow chart in Fig. B1. Almost the entire computational effort is carried out in blocks A and B, with the computation in block B being performed on a mode-by-mode basis. In this block, at every interface, the pressure field to the left of the interface is projected onto the mode set in the next segment, producing the excitation coefficients. These are in turn immediately used to build the finely-sampled pressure field at the end of the segment necessary to repeat this procedure at the subsequent interface. Also the mode amplitudes at the desired receiver depths are retained to enable the computation indicated in the subsequent block.

3

Installation of C-SNAP

C-SNAP is written in VAX Fortran and runs under the VAX/VMS operating system. Due care has been taken to enhance its portability, with the number of deviations from the standard Fortran 77 being minor and usually supported on systems other than the VAX, such as the use of the INCLUDE statement. C-SNAP is implemented at SACLANTCEN on a VAX 6000 computer, as well as on a number of workstations and personal computers. The code produces either printed or plotted outputs. In the latter case we use the two SACLANTCEN standard plotting packages FIPLOT and CONTUR, which are common to a number of SACLANTCEN models. Compilation and linking in a VAX/VMS environment is obtained through the command file C-SNAP.CLK shown in Fig. B2.

C-SNAP uses a number of include files in order to consistently control the array sizes throughout the various program units. The main parameters determining the program size, defined in the include file PARAM.INC, are the maximum number of modes to be computed (MODEN), and the maximum number of depths allowed for propagation loss calculations (MAXND). The default size is set to a maximum of 500 modes and 501 depths. The resulting virtual memory requirement is of the order of 6 Mbytes in a VAX/VMS environment. The test cases shown in this memorandum have also been run on a personal computer.

4

Running C-SNAP

The description of the environment and of the required computational outputs must be supplied through an input file with name `C-SNAP.DAT`. All the output files have the unique filename `C-SNAP` and are distinguishable by their extensions only. Their definition is in subroutine `FILE.FOR`. However, full flexibility in choosing input and output filenames is conveniently achieved by renaming the `C-SNAP` filenames by means of the command file used to start the execution of the code. The content of this command file named `C-SNAP.COM` is shown in Fig. B3. As an example, the command for running `C-SNAP` with the input file `CASE1.DAT` is

```
$ @C-SNAP CASE1
```

and the resulting output files are identified as follows:

`CASE1.PRT` Contains all the printed output.

`CASE1.PLP` Contains plotting parameters (axes, labels, etc.) for the 2-D plots possibly required (`MODES`, `PROFL`, `TLRAN`, `TLDEP`).

`CASE1.PLT` Contains the actual data to be plotted.

`CASE1.CDR` Contains contour parameters (`CONDR`).

`CASE1.BDR` Contains the actual contour data.

4.1. INPUT STRUCTURE

We have adopted the input structure used for `SUPERSNAP`, which in turn is almost identical to that used for the adiabatic range-dependent version of `SNAP` [1]. However, a few differences are unavoidable, either because new parameters need to be specified (such as the number of range subdivisions required to approximate a sloping bottom or a range-varying sound-velocity profile, and the range coordinate of every new input profile), or because some former input parameter (such as the number of discretization points to be used to compute the eigenfunctions) is now estimated by the code and can be removed from the input stream.

4.2. ENVIRONMENTAL INPUTS

A summary of the environmental inputs is shown in Table/Figure C1 in Appendix C. All the inputs are read through a list-directed Fortran statement, with every row in the table indicating an input record. Parameters belonging to the same record must be separated by either commas or blanks and may be supplied by using more than one line. Each of the various input profiles required to describe a range-dependent environment must always initiate with the input record [H0, S0, S1, RB, N2] and terminate with the input record [B2S, C2S]. The last input profile is considered to extend in range, with constant properties, just as far out as necessary to complete the transmission loss calculations. As an immediate consequence we observe that if only one profile is given in the input, C-SNAP will treat the case as a range-independent problem. The maximum number of environments which can be handled by the present program version, i.e. the number of input profiles plus the number of range subdivisions, is 8193. The following is a detailed description of the environmental inputs:

TITLE Title of run that will appear as the heading on all printed and plotted outputs.

NF Number of source frequencies.

F(1) . . . F(NF) Source frequency in Hz. Frequency values can be given in any order, but the program will start execution from the lowest frequency.

MIN, MAX, MPROP

MIN Minimum order mode to be included in the source field.

MAX Maximum order mode to be included in the source field. Actually, the maximum order mode in the source field will be the minimum between this parameter and:

- The array size limit defined through the parameter MODEN.
- The highest-order mode existing for the particular environment, determined by C-SNAP.

MPROP Maximum order mode to be included in the propagating field. This parameter is used to establish the higher bound for the modes which enter into the coupling process.

For example, with the parameter MODEN set to 500, in the usual case where the full mode set must be included in the source field and propagated out in range, a convenient choice for the parameters MIN, MAX, and MPROP would be 1, 500, and 500.

On the other hand, in the case where a particular study requires the investigation of the propagation effects due to the source field resulting from a subset of the full mode set, for instance from the first 10 modes only, by setting MIN, MAX, and MPROP

to 1, 10, and 500, then the source field from the first 10 modes will be allowed to couple at every interface with the full set of the local modes.

MSP, ERMAX

MSP Controls the vertical grid size to be used to display the acoustic field over depth. It applies to options CONDR and TLDEP only. The grid size is determined as: $G\text{SIZE}=(H0/MSP)$ with $H0$ being the water depth of the first profile. $G\text{SIZE}$ is maintained constant over range and applies to both water and bottom layers. Specifying a zero value for MSP will result in the default choice $MSP=50$, which is a reasonable choice for shallow water environments.

It is worth noting that C-SNAP automatically determines the number of vertical points required for accurately solving the wave equation. However, this number is generally much larger than the number of grid points necessary to display the acoustic field over depth. MSP can be seen as a sampling over the many points used for solving the wave equation.

ERMAX Accuracy parameter influencing the eigenvalues. The criterion adopted is to compute the eigenvalues with sufficient accuracy to ensure modal phase errors smaller than a wavelength at a range of $ERMAX$ km. The default value is $ERMAX=0$, which activates a pre-established accuracy criterion. For maximum accuracy specify $ERMAX=10^{38}$.

H0, S0, S1, RB, N2

H0 Thickness of water layer in meters. This layer can be omitted, with the exception of the first input profile, by setting $H0$ equal to zero. In this case the profile must be omitted. To simplify the numerical procedures in C-SNAP this case is treated by introducing an artificial 1 mm water layer with sound speed taken at the corresponding depth from the previous input profile.

S0 Rms roughness of the sea surface in meters.

S1 Rms roughness of the seafloor in meters.

RB Range in km at the beginning of the current input profile. This parameter must be set equal to zero for the first profile. All the environmental properties are assumed constant beyond the maximum input range.

N2 Parameter to control the number of range subdivisions to be introduced in the interval from the starting of the current input profile until the end of the subsequent one. $N2$ may assume both negative and positive integer values. For zero or positive values of $N2$ the environment in the interval between the two profiles is approximated by generating $(2^{N2} - 1)$ equidistant profiles obtained through linear interpolation in range. All the profiles in the interval identify a range-independent segment with interfaces set exactly at the midpoint between any two profiles. The result of the above criterion for range subdivisions is already shown in Fig. A2.

As an example, if $N2$ is set equal to zero, then no additional profile is introduced between the two input profiles, and only one coupling interface will exist, occurring at a range exactly midway between the two input profiles.

Again as an example, by setting $N2$ equal to one, then one profile is introduced, located midway between the two input profiles, and two coupling interfaces will exist, located at $1/4$ and $3/4$ of the interval between the two input profiles.

For negative values of $N2$ all the properties in the current profile are maintained as in a perfectly range-independent environment until a new input profile is reached. The new coupling interface will occur at the start of the new input profile.

Though the parameter $N2$ has an effect only between any two consecutive input profiles, for consistency in the input structure it must be specified for the last input profile as well.

$Z0(I)$, $C0(I)$ Sound-speed profile in the water column. The first value given must be at the sea surface ($Z0(1)=0$) and the last value at the seafloor ($Z0(M)=H0$). If $H0$ is equal to zero, the profile must be omitted.

$H1$, $R1$, $B1$

$H1$ Thickness of sediment layer in meters. This layer can be omitted by setting $H1$ equal to zero. In this case the profile must be omitted, while $R1$ and $B1$ are dummy, and can be omitted as well.

$R1$ Density of sediment in g/cm^3 .

$B1$ Compressional wave attenuation in sediment in dB/λ .

$Z1(I)$, $C1(I)$ Sound-speed profile in the sediment layer. The first value given must be at the water/sediment interface ($Z1(1)=0$) and the last value at the sediment/subbottom interface ($Z1(N)=H1$). Normally there will be a discontinuity in the profile at the water/sediment interface, i.e. $C0(M) \neq C1(1)$.

$R2$, $B2$, $C2$

$R2$ Density of subbottom in g/cm^3 .

$B2$ Compressional wave attenuation in subbottom in dB/λ .

$C2$ Compressional speed in subbottom in m/s . A necessary condition for discrete modes to exist is that this speed be higher than the minimum speed in both water and sediment.

$B2S$, $C2S$

$B2S$ Shear wave attenuation in subbottom in dB/λ . By treating the subbottom as a 'Voigt' solid [9], we impose upper limits on both shear attenuation ($B2S <$

$0.75 \times B2(C2/C2S)^2$) and shear speed ($C2S < \sqrt{0.75 \times C2}$).

- C2S** Shear speed in subbottom in m/s. Shear wave can be neglected by putting C2S equal to zero. In this case the attenuation B2S becomes a dummy parameter. Since the effect of shear waves is introduced in a perturbational approach, C2S has to be small compared with the compressional speed C1(1) for results to be accurate ($C2S < 600$ m/s).

4.3. CHANGING DEFAULT PARAMETERS

The development and testing phases of this program have required the tuning of some default parameters as well as the analysis of some particular effects. This was obtained by controlling the program flow through the use of input code words. We believe this feature may still have a value and consequently the code word structure is maintained (Table/Figure C2). Here we give the rules governing the specification of these 'new default' code words:

- If a new default code word is used, it must initiate after the last environmental section is terminated and must precede the first computational input specification. Their order and the number is not relevant.
- Each code word is composed of five uppercase characters, with the first character always starting from column one. If a numerical value must be given as well, then it must be supplied on the same line as the code word using a list-directed format. The occurrence of a numerical value is shown in Table/Figure C2 as a lowercase three-character string.
- A code word is ignored when preceded by an exclamation mark in column one. A list of option codes can be kept in the input file and their effect activated or deactivated according to the use of the exclamation mark.
- Their effect is extended to all the computational outputs whenever meaningful.

4.4. COMPUTATIONAL INPUTS

The basic building blocks required to identify the computational inputs consist of a sequence of lines with either code words, or numerical values, or a mixture of the two. The code words are used to define the required output options, the calculation type and the preferred output type. Code words are also used to define plot axes; in this case four or five numerical values need to be specified on the same line. Finally, lines with numerical values only are used to define source depths, receiver depths, range intervals and increments. As a general rule, all the code words must be given in uppercase letters. Also as a rule, the lowercase character strings appearing throughout this section on the same line as some of the code words, should be replaced with numerical values supplied through a list-directed format. The computational inputs must follow immediately after the last 'new default' code word.

4.4.1. *Output options, calculation, and output type code words*

These code words must be given on the same input line, with the output option coming first starting from column one, followed by a choice of the calculation and output code words in any order, each separated by a single blank character or a comma. As illustrated in Table/Figure C3, they consists of either five- or three-character uppercase strings. Though in principle their association is intended to be as free as possible, in practice there are some limitations. For instance, the code words COH and INC are meaningless in conjunction with option PROFL and MODES, while the code word PRT is not allowed in connection with the output option CONDR as it would generate too large a print file. By default, the output type for the CONDR and PROFL output options is set to PLT. Table/Figure C4 shows the allowed combinations of the above code words.

4.4.2. *Plot axis code words*

They consist of five uppercase character strings, with the first character in column one, and followed on the same line by four or five numerical values as shown in Table/Figure C5. Three-dimensional plots are produced for option CONDR with contour lines. In this case the third axis (ZAXIS) is used to indicate the contour levels and the number of smoothings required. Also a two-dimensional smoothing of the loss surface is available and is performed by the contour package. The specification of the plot axes is optional. If omitted, the default values shown in Table/Figure C6 are used instead. Also, within this group of code words there is no order of precedence.

4.4.3. *Grouping of computational input lines*

The complete specification of each output option is obtained through the grouping of a fixed sequence of the computational input lines. The order of each group of lines in the input run stream is entirely free. Input lines requiring only numerical values may not be omitted. A summary of each group is illustrated in Tables/Figures C6a-d.

4.5. *NUMERICAL CONSIDERATIONS*

C-SNAP automatically determines the density of the vertical grid used for solving the wave equation. The algorithm consists in estimating the maximum number of discrete modes in the problem and then associating eight points per mode as the initial mesh density. The initial solution for the wave number is progressively refined over a sequence of increasingly denser meshes (a total of four meshes is used as a default choice) and the results are finally extrapolated to yield the solution of the wave number for an infinitely dense mesh. The computation of the mode coefficients is performed by using the mode amplitudes obtained on the first mesh. Table/Figure C2 lists a number of computational sub-options which allow deviation from the above default choice in case it is desired either to push the code to extreme accuracy or to trade accuracy in favour of speed.

In our experience covering a large variety of cases in range-independent environments, the above procedure has generally been quite satisfactory in producing an accurate result of the pressure field over long propagation ranges. However, in range-dependent environment, the convergence of the model output is clearly influenced by the choice of the number of range subdivisions, with this quantity being related both to the change in bathymetry and to the source frequency. A simple technique in this case consists in running C-SNAP with increasing values for the input parameter N2 until a stable solution is found.

5

Examples

The use of C-SNAP and the comparison with other range-dependent models is illustrated for the following three test problems:

1. Propagation upslope in a wedge-shaped waveguide with a lossy penetrable bottom.
2. Propagation downslope in a wedge-shaped waveguide with a lossy penetrable bottom.
3. Deep water propagation over a seamount.

In the first two test cases the reference solution has been obtained from COUPLE by using the impedance matching condition at the coupling interfaces. For test case 3, our reference solution has been obtained from IFDPE [10] and for consistency with the approach taken in this model we have run C-SNAP using reduced-pressure matching [8].

5.1. CASE 1 – UPSLOPE PROPAGATION IN A WEDGE-SHAPED WAVEGUIDE

As shown in Fig. A3, the environment consists of a homogeneous water column ($c_1 = 1500$ m/s, $\rho_1 = 1$ g/cm³) limited above by a pressure-release flat sea surface and below by a sloping seafloor. The bottom is a homogeneous fluid halfspace with a compressional speed of 1700 m/s, a density of 1.5 g/cm³, and an attenuation of 0.5 dB/ λ . In order to take into account the contribution from the continuous spectrum in the near field we have introduced a 4000 m false bottom. The water depth at the source position is 200 m, while the wedge apex occurs at a distance of 4 km from the source resulting in a slope of approximately 2.86°. In this problem we have a 25 Hz CW source placed at mid-depth (100 m) and two receivers at 30 and 150 m depth. The selected receiver depths provide samples of the acoustic field in the water column as well as in the bottom. The reference solution has been obtained with COUPLE [11] and is already reported [12]. The input run stream used to solve this case with C-SNAP is shown in Fig. B4.

The propagation loss plots for the two receivers presented in Fig. A4 show excellent results for the receiver at 30 m but not as good for the receiver at 150 m. We explain this fact by observing that:

- The eigenfunctions are obtained through algorithms which use real arithmetic

and their solution becomes approximate in the presence of loss. To get the exact solution, complex calculations should be used instead, at the expense of a less robust algorithm and more CPU time.

- While the influence of bottom loss on the waterborne modes is practically insignificant (water is a relatively low loss region), the opposite occurs for the bottom-bounce modes as they have a large oscillatory size in the bottom layer. Though these bottom-bounce modes usually carry little energy, they are essential for mode coupling. The effect of inaccurate bottom-bounce modes in range-independent environments is rarely observed as no mode coupling is required and these modes decay rapidly out in range.
- While the 30 m receiver hits the bottom only at a range of 3.4 km, the 150 m receiver will lie in the sediment (lossy layer with the pressure field represented by the bottom-bounce modes) starting at a range of 1 km, which is exactly the range where the agreement deteriorates.

As a final comment we report that the comparison of COUPLE and C-SNAP results obtained after removing the attenuation loss from the sediment layer shows excellent results for both receiver depths.

5.2. CASE 2 – DOWNSLOPE PROPAGATION IN A WEDGE-SHAPED WAVEGUIDE

The geometry of this problem is illustrated in Fig. A5. The initial water depth is 100 m and increases linearly to 1000 m at a range of 4 km, resulting in a downslope wedge with an angle of 12.7° . The sound speed in the water column is 1500 m/s, while in the bottom the sound speed is 1700 m/s, the density is 2 g/cm^3 and the attenuation is $0.5 \text{ dB}/\lambda$. We compute propagation losses for a 100 Hz line source in plane geometry located at 50 m depth. Also, we limit the starting field to the first 6 discrete modes (this is the maximum number of evanescent modes in the sediment layer), we introduce a false-bottom depth of 4000 m, and allow for a maximum of 160 modes in the propagating field, roughly corresponding to an angle of 45° . The input run stream used to run C-SNAP is shown in Fig. B5.

We illustrate in Fig. A6 the comparison of the propagation loss over the water column obtained from COUPLE and C-SNAP at a range of 4 km. Though the two curves show a generally good agreement, still we observe differences of about 3 dB around a depth of 50 m. Similar to the findings for test case 1, further investigation has shown that we get excellent agreement when removing the bottom attenuation loss of $0.5 \text{ dB}/\lambda$. Since in a downslope situation this disagreement cannot be attributed only to the bottom interaction of the discrete spectrum of the pressure field, we come to the conclusion that the problem is associated with the oversimplification adopted in mathematically describing the continuous-spectrum modes, i.e. their treatment with real arithmetics is not adequate for the purpose of mode coupling in a lossy medium.

To give further evidence to this conclusion we have run this case at a lower frequency in order to increase the influence of the lossy bottom. The results are shown in Fig. A7 where we compare COUPLE and C-SNAP propagation losses versus range for a frequency of 25 Hz and a receiver depth of 50 m. While in this case we see differences up to about 10 dB, we note that the comparison for the lossless case at 25 Hz gives excellent agreement for both downslope and upslope propagation.

It is also worth noting that the evidence of a larger disagreement in the near-surface region may well be explained by considering that the energy in the near boundary regions strongly depends on the high-order modes, that is on the modes which have a stronger interaction with the lossy bottom.

5.3. CASE 3 – DEEP WATER PROPAGATION OVER A SEAMOUNT

Here we test the model along a 200 km deep-water track where the range dependence is obtained through a combination of upslope and downslope environments so as to build an idealized seamount. We limit in this case the modal starting field to retain only those modes which are waterborne, thus facilitating the comparison with the IFDPE [10] narrow-angle PE code. The environment is illustrated in Fig. A8. The input runstream used for running C-SNAP is shown in Fig. B6.

The contoured propagation losses versus depth and range for a frequency of 50 Hz and a source depth of 100 m is shown in Fig. A9. This plot shows a convergence zone type pattern with a beam of energy cycling up and down the water column until at a range of about 90 km the beam hits the seamount and reflects at steeper angles. This result is practically indistinguishable from the same one obtained from the IFDPE. As shown in Fig. A10 we have excellent agreement also for a single source/receiver depth combination.

5.4. NUMERICAL PARAMETERS AND CPU TIMES FOR CASES 1, 2, AND 3

The CPU times shown in the following table refer to a VAX 9000 computer which is roughly a 22 Mflops machine.

All the existing modes at the source range have been included in the starting field, except as noted in case 3 where the source field is produced with the waterborne modes only. To save execution time with C-SNAP we have used in all three cases the sub-option code word OPTMZ. In this case C-SNAP automatically limits the number of modes in the propagating field by discarding modes carrying insignificant energy.

Further improvement in coupled mode approach could be obtained by:

- Introducing a more accurate treatment of the continuous-spectrum modes in lossy environments.

- Including a deep absorbing layer in order to remove undesired returns from the false bottom, and hence permit a reduction of the false-bottom depth.
- Using coupled wedge modes [13].

The code could also take advantage from parallel processing.

Table 1 *Numerical parameters and CPU times for the various test cases*

Test case	Model	DZ (m)	DR (m)	Range subdiv	ZMAX (m)	CPU time
1	C-SNAP	(1)		65	4000	2 min
	COUPLE			65	4000	27 min
2 100 Hz	C-SNAP			129	4000	33 min
	COUPLE			129	4000	7 h 37 min
2 25 Hz	C-SNAP			129	4000	14 min
	COUPLE			129	4000	1 h 30 min
3	C-SNAP	6.84	20	67	(2)	5 min
	IFDPE			7000	7000	2 min

¹ DZ is automatically determined by C-SNAP and COUPLE.

² No false bottom.

6

Conclusions

We have described a range-dependent coupled mode program with the following features:

- (a) Solves for the outgoing travelling component of the wave equation by means of a robust and efficient algorithm using real arithmetic.
- (b) Includes loss in a perturbational approach.
- (c) Accounts for energy conservation at horizontal boundaries by applying an impedance matching technique.
- (d) Has a built-in algorithm for choosing the vertical grid required to obtain an accurate solution of the wave equation.
- (e) Treats bathymetric changes through a stair step approximation of range-independent segments.
- (f) The search for a stable solution is limited to the definition of the number of range subdivisions.
- (g) Gives an accurate description of the pressure field in lossless media and more in general whenever the bottom-bounce modes are adequately described.
- (h) Execution speed is relatively fast, and the overall time required to get a stable solution is mainly dependent on the choice of a single parameter: the number of range subdivisions.
- (i) Available for both VAX and PC computers.

References

- [1] Jensen, F.B. and Ferla, C.M. SNAP: The SACLANTCEN normal-mode acoustic propagation model, SACLANTCEN SM-121. La Spezia, Italy, NATO SACLANT Undersea Research Centre, 1979. [AD A 067 256]
- [2] Porter, M.B. The KRAKEN normal mode program, SACLANTCEN SM-245. La Spezia, Italy, NATO SACLANT Undersea Research Centre, 1991. [AD A 252 409]
- [3] Porter, M.B., Ferla, C.M. and Jensen, F.B. Coupled modes for rapid range-dependent modeling. *In*: Lee, D., Vichnevetsky, R. and Robinson, A.R., eds. Computational Acoustics: Proceedings of the 3rd IMACS Symposium on Computational Acoustics, Cambridge, MA, 26–28 June 1991. Volume 2. Amsterdam, North-Holland, 1993: pp. 307–316. [ISBN 0 444 89762 3]
- [4] Porter, M.B. and Reiss E.L. A numerical method for bottom interacting ocean acoustic normal modes, *Journal of the Acoustical Society of America* **77**, 1985: 1760–1767.
- [5] Evans, R.B. A coupled mode solution for acoustic propagation in a waveguide with stepwise depth variations of a penetrable bottom, *Journal of the Acoustical Society of America* **74**, 1983: 188–195.
- [6] Collins M.D. and Westwood, E.K. A higher order energy conserving parabolic equation for range-dependent ocean depth, *Journal of the Acoustical Society of America* **89**, 1991: 1068–1075
- [7] Collins, M.D. A split step Padé solution for the parabolic equation method, *Journal of the Acoustical Society of America* **93**, 1993: 1–7.
- [8] Porter, M.B., Jensen, F.B. and Ferla, C.M. The problem of energy conservation in one-way models, *Journal of the Acoustical Society of America* **89**, 1991: 1058–1067.
- [9] Kolsky, H. Stress Waves in Solids. New York, NY, Dover Publications, 1963.
- [10] Lee, D. and Botseas, G. An implicit finite-difference computer model for solving the parabolic equation, NUSC TR-6659. New London, CT, Naval Underwater Systems Center, 1982. [AD A 117 701]
- [11] Evans, R.B. COUPLE: a user's manual, NORDA TN-332. NSTL Station, MS, Naval Ocean Research and Development Activity, 1986. [AD B 106 858]
- [12] Jensen F.B. and Ferla, C.M. Numerical solutions of range-dependent benchmark problems in ocean acoustics, SACLANTCEN SR-141. La Spezia, Italy, NATO SACLANT Undersea Research Centre, 1988. [AD B 131 373]
- [13] Primack, H.P. and Gilbert, K. A two-dimensional model based on coupled wedge modes, *Journal of the Acoustical Society of America* **90**, 1991: 3254–3262.

Appendix A

Graphical illustration of the
geometry for the three test cases
and comparison of the results

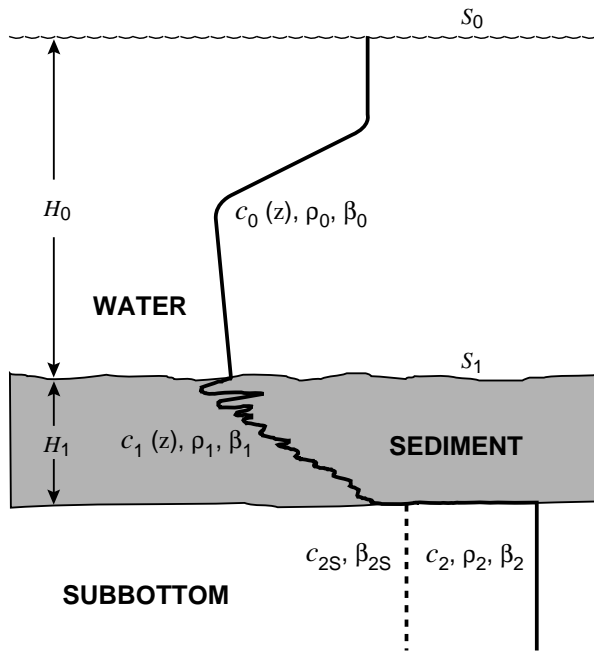


Figure A1 Propagation media handled by C-SNAP.

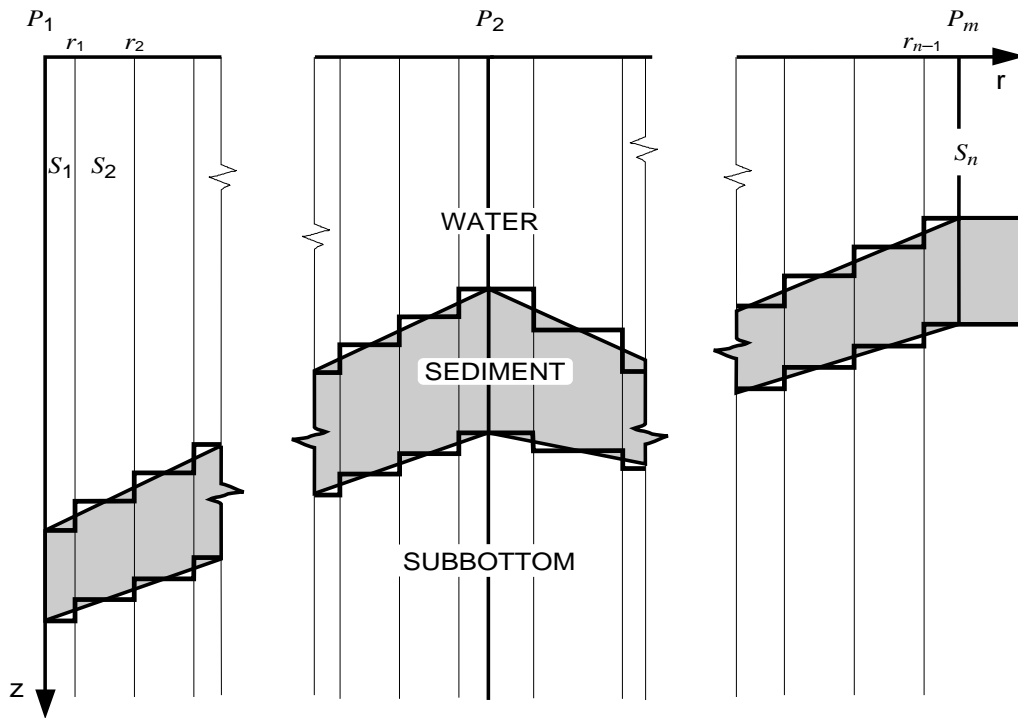


Figure A2 Stair step approximation of sloping bottom environment.

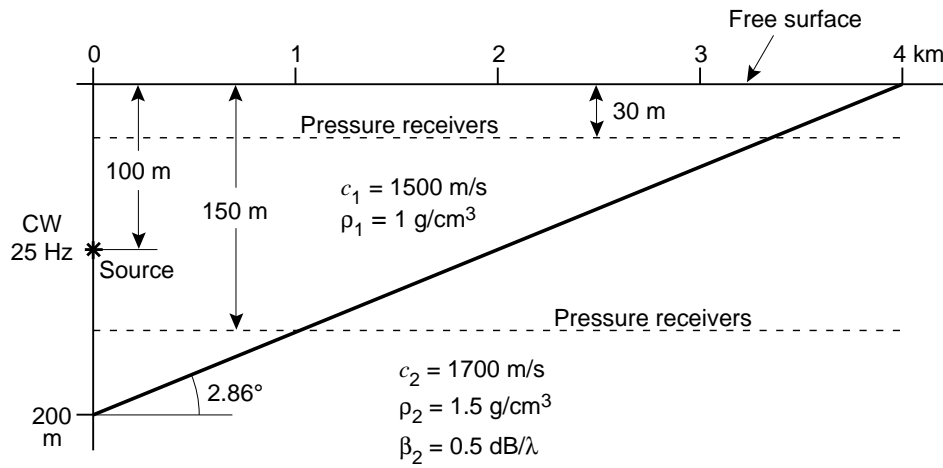


Figure A3 *Wedge geometry for case 1, upslope propagation.*

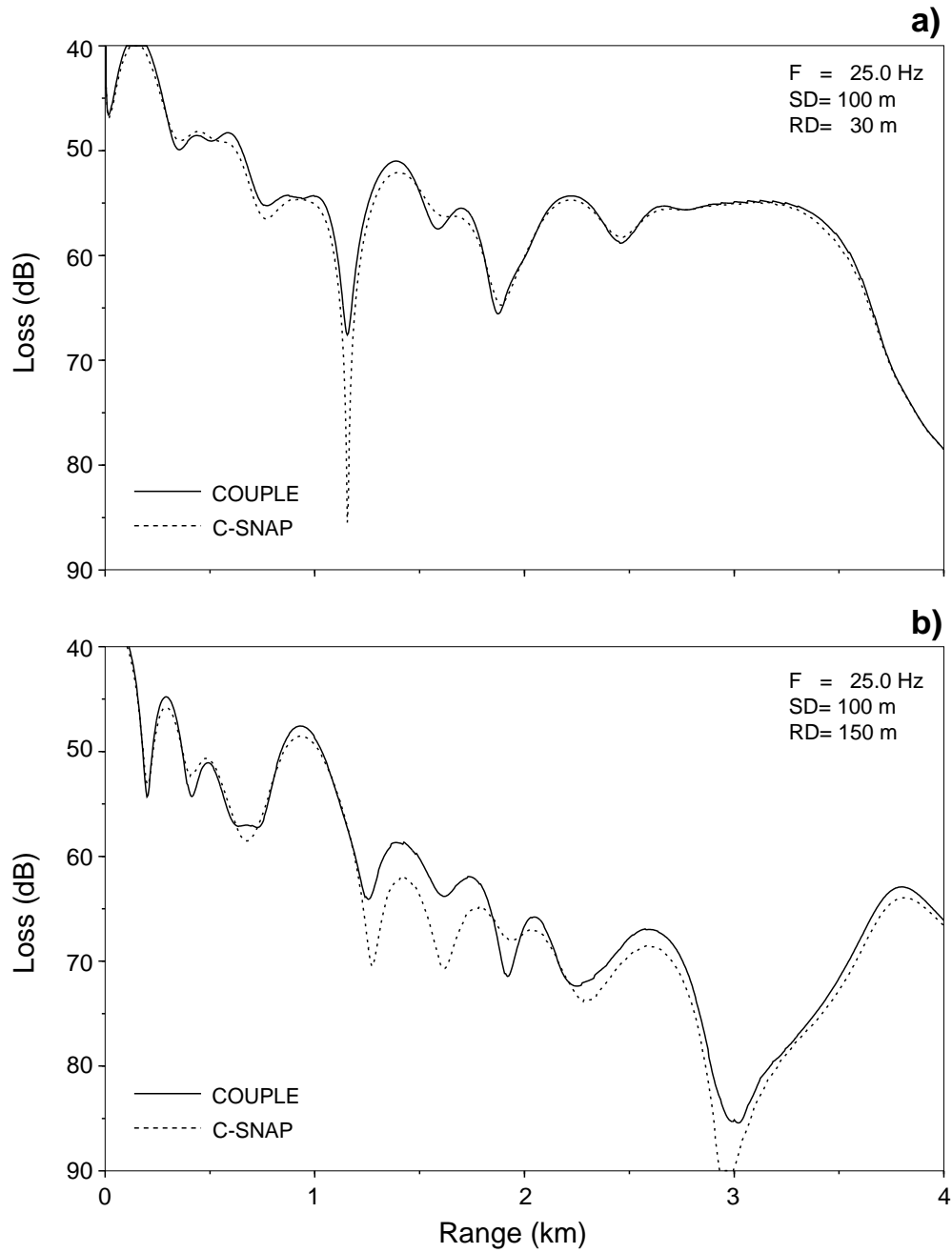


Figure A4 Comparison of one-way results from COUPLE and C-SNAP for case 1 (a) receiver at 30 m; (b) receiver at 150 m.

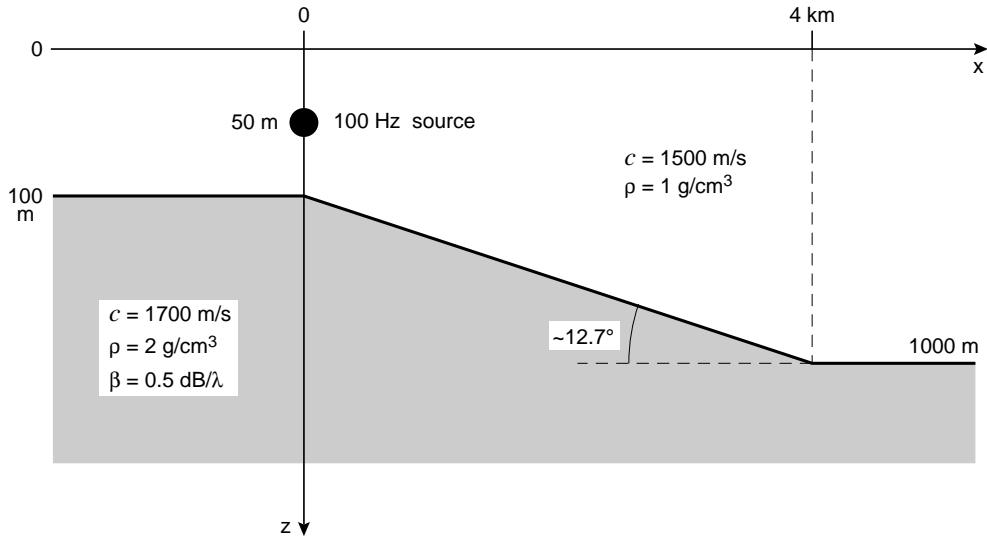


Figure A5 Wedge geometry for case 2, downslope propagation.

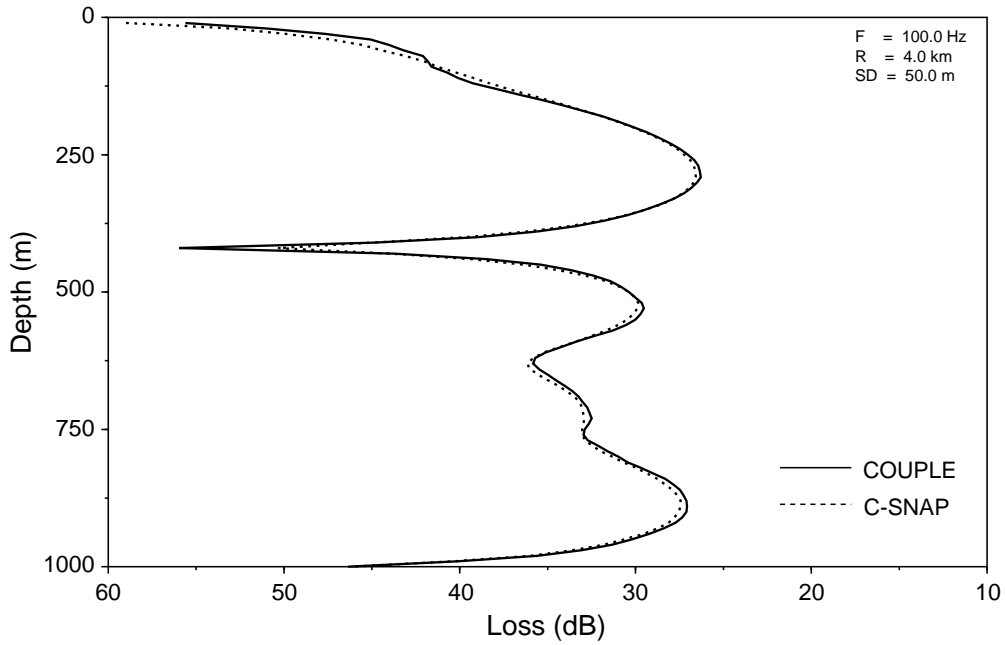


Figure A6 Comparison of one-way results from COUPLE and C-SNAP for case 2; 100 Hz source, loss versus depth.

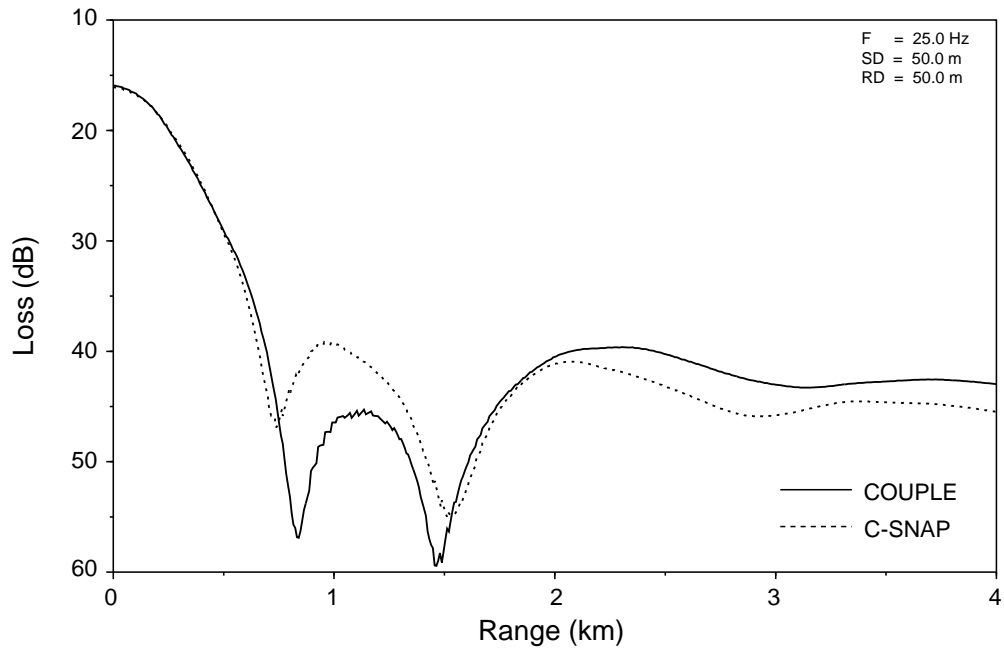


Figure A7 Comparison of one-way results from COUPLE and C-SNAP for case 2, 25 Hz source, loss versus range.

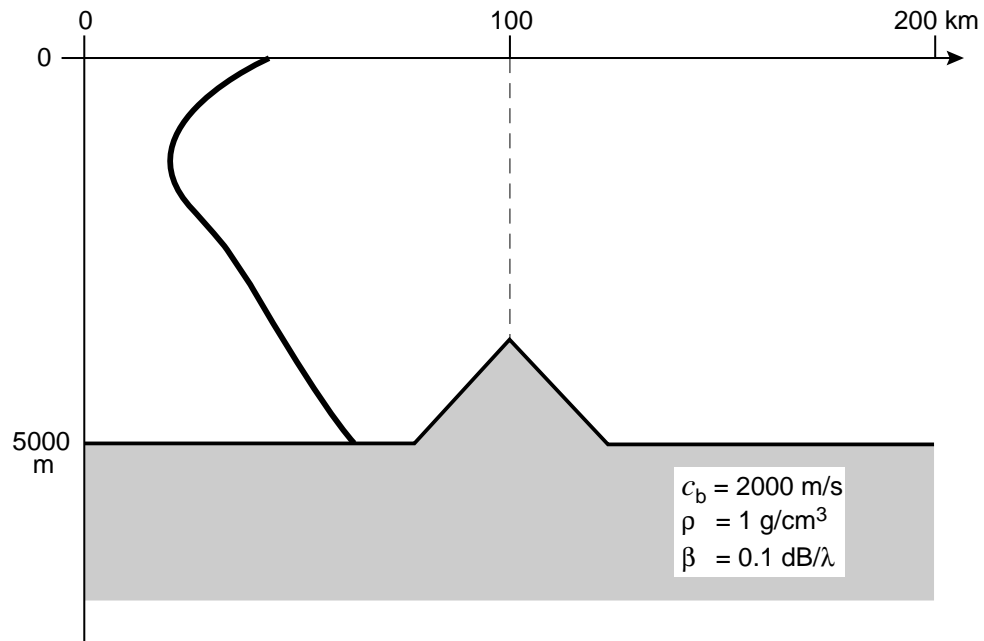


Figure A8 Schematic of the seamount problem in case 3.

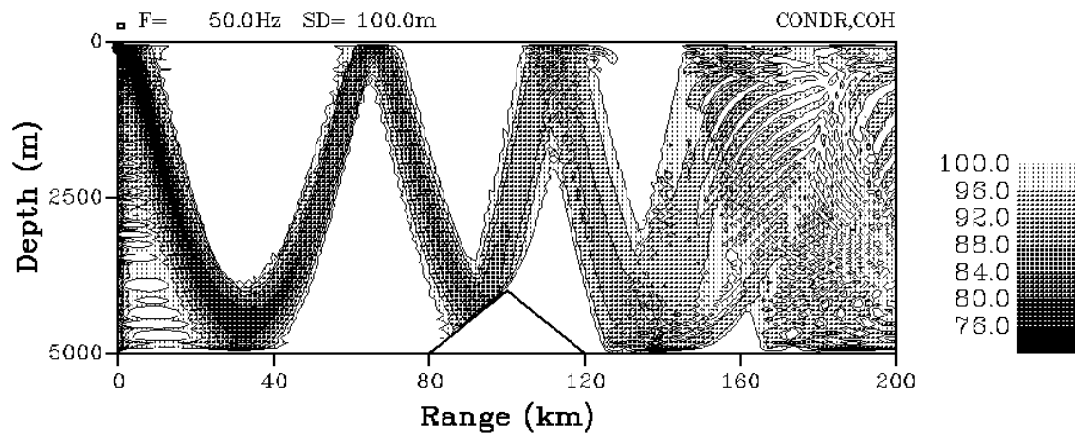


Figure A9 C-SNAP field versus depth and range for the seamount problem in case 3.

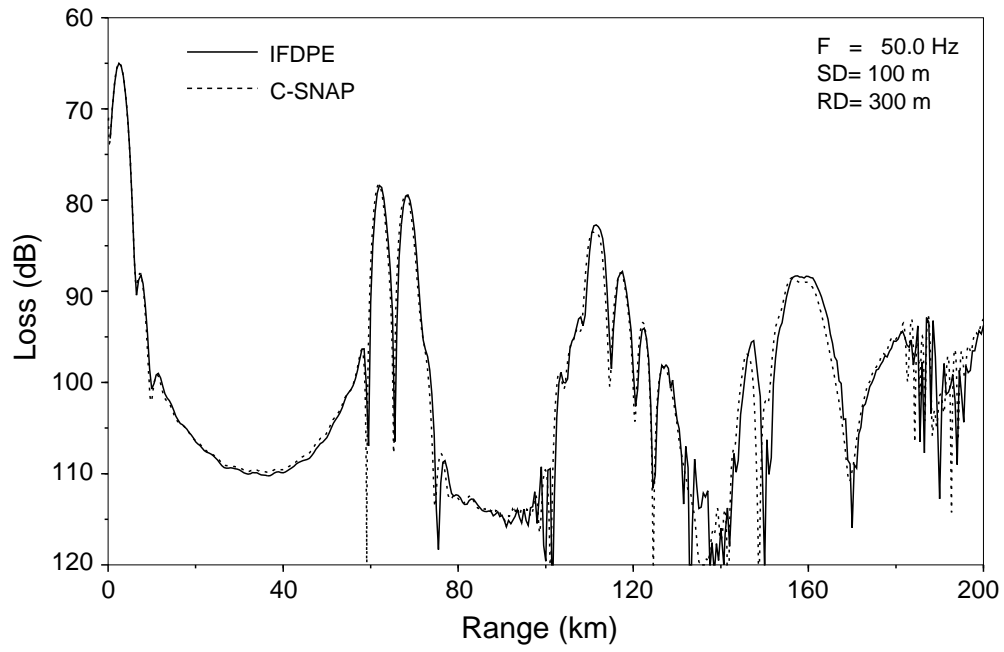


Figure A10 Comparison of one-way results from C-SNAP and IFDPE for case 3.

Appendix B

Program structure, command files, and
input runstreams for the three test cases

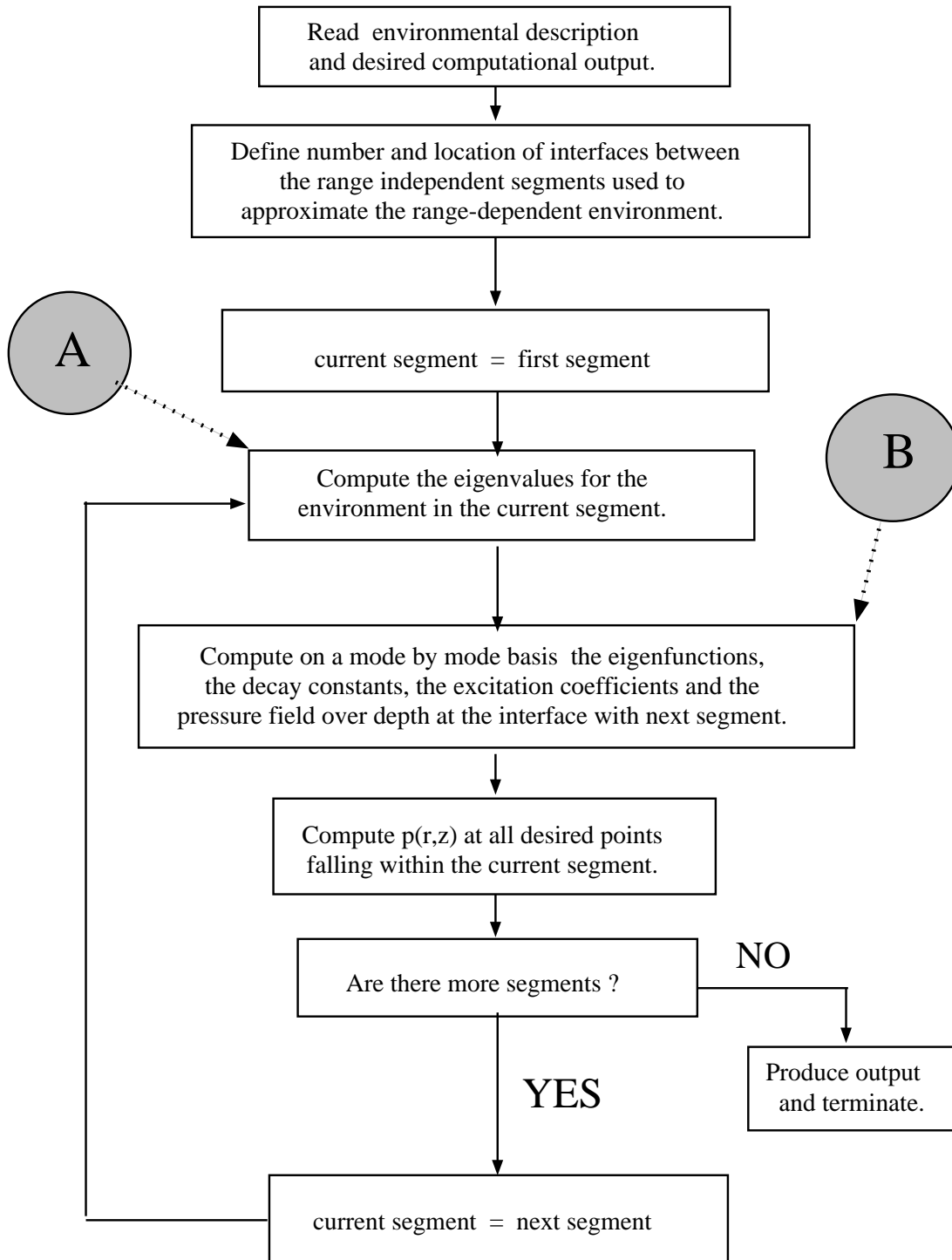


Figure B1 *First level structure of C-SNAP.*

```
$ FOR                                MAIN, -
    ACCRCY, -
    BLKDAT, BRENT, -
    CHARAC, CHKOPT, COMPUTE, CONDRC, CONVRG, CZS, -
    DEFSO, -
    EIGVEC, EVALCM, -
    FILE, FNDVEC, FIRSTP, -
    GET_HDR, GETIME, GETONE, -
    INIT, INPUT, IPULSE, ISITAN, ISOBR, ISOINT, -
    JOIN, LAGCMP, LAGRANGE, -
    MDIAG, MESHES, MODE, MODES, MODHDR, MODPRT, -
    NEWENV, NEWMOD, NEWPRO, NEWTON, NR122, NR142, -
    OUTPL, OUTSUM, -
    PEKRT, PLEFT, PLEFTR, PLEFTS, PLTFILE, PORTER, -
    PROFL, PROFL_RI, PROF_EQV, PROF_INT, -
    RDALFA, RDIV, RDNUMB, RDSO, REFL1, RETRV, REVISE, RFFORM, -
    START, STATIST, STURM, -
    TLCPL, TLDEP_CP, -
    VELOCITY, -
    WEIGHT, -
    ZSMPL
$ libr/create/in                    C-SNAP -
    ACCRCY, -
    BLKDAT, BRENT, -
    CHARAC, CHKOPT, COMPUTE, CONDRC, CONVRG, CZS, -
    DEFSO, -
    EIGVEC, EVALCM, -
    FILE, FNDVEC, FIRSTP, -
    GET_HDR, GETIME, GETONE, -
    INIT, INPUT, IPULSE, ISITAN, ISOBR, ISOINT, -
    JOIN, LAGCMP, LAGRANGE, -
    MDIAG, MESHES, MODE, MODES, MODHDR, MODPRT, -
    NEWENV, NEWMOD, NEWPRO, NEWTON, NR122, NR142, -
    OUTPL, OUTSUM, -
    PEKRT, PLEFT, PLEFTR, PLEFTS, PLTFILE, PORTER, -
    PROFL, PROFL_RI, PROF_EQV, PROF_INT, -
    RDALFA, RDIV, RDNUMB, RDSO, REFL1, RETRV, REVISE, RFFORM, -
    START, STATIST, STURM, -
    TLCPL, TLDEP_CP, -
    VELOCITY, -
    WEIGHT, -
    ZSMPL
$!
$ LINK/EXE=C-SNAP                    MAIN, C-SNAP/LIB
```

N.B.: At compilation time the following (INCLUDE) files must also be available:
PARAM.INC, ACOMMON.INC, BCOMMON.INC, COMMON.INC.

Figure B2 C-SNAP.CLK: *command file to compile and link.*

```
$
$ COPY      'P1' .DAT          C-SNAP.DAT
$!
$ RUN  C-SNAP
$!
$ RENAME C-SNAP.PLP      'P1' .PLP
$ RENAME C-SNAP.PLT      'P1' .PLT
$ RENAME C-SNAP.CDR      'P1' .CDR
$ RENAME C-SNAP.BDR      'P1' .BDR
$ RENAME C-SNAP.PRT      'P1' .PRT
$!!!!
$ @PLOT 'P1'
$ @CONTUR 'P1'
```

NOTE : The commands "PLOT" and "CONTUR" will chain the execution of the plotting packages.

Figure B3 C-SNAP.COM: *command file for running the code.*

SACLANTCEN SM-274

WEDGE-SHAPED WAVEGUIDE

```
1
25.
1 90 90
100, 0
200. 0. 0. 0. 6 ! REG 1
0. 1500.
200. 1500.
3800. 1.5 0.5
0. 1700.
3800. 1700.
1.5 0.500 1.0E10
0. 0.
0.0 0. 0. 4.0 0 ! REG 2
4000.0 1.5 0.5
0. 1700.
4000.00 1700.
1.5 0.500 1.0E10
0. 0.
NMESH 1
OPTMZ
TLRAN,COH,PLT
XAXIS 0., 4., 12., 1.
YAXIS 40. 90. 7.5 10.
0. 4. 0.005
100. 30.
100. 150.
CONDR,COH,COL
XAXIS 0 4 16 1
YAXIS 0 300 10 50
ZAXIS 40 67 3
0 4 0.02
100.
@EOF
```

Figure B4 *Input run stream for case 1.*

```

DOWNSLOPE WEDGE, 12.7 degrees, IMPEDANCE MATCHING
1
100.
1 6 160
10, 0
100. 0. 0. 0. 7 ! REG 1
0. 1500.
100. 1500.
3900.0 2.0 0.500
0. 1700.
3900. 1700.
2.0 0.500 1.0E10
0. 0.
1000. 0. 0. 4. 0 ! REG 2
0. 1500.
1000. 1500.
3000. 2.0 0.500
0. 1700.
3000. 1700.
2.0 0.500 1.0E10
0. 0.
!OPTMZ
NMESH 1
PLANE
TLDEP,COH,PLT
XAXIS 10 60 16 10
YAXIS 0 1000 10 250
4. 4. 0.
50
TLRAN,COH,PLT
XAXIS 0., 4., 16., 1.0
YAXIS 10 60 10 10
0. 4.0 0.004
50. 50.
@EOF

```

Figure B5 *Input run stream for case 2.*

SACLANTCEN SM-274

DEEP WATER PROPAGATION OVER A SEAMOUNT, REDUCED PRESSURE MATCHING

```
1
50
1 62 100
100 0
5000.0 0.0 0.0          0          -1      ! Profile 1
  0.0, 1536.00
  200.0, 1528.00
  700.0, 1502.00
  800.0, 1500.00
 1200.0, 1497.00
 1500.0, 1497.00
 2000.0, 1500.00
 3000.0, 1512.00
 4000.0, 1528.00
 5000.0, 1545.00
  0.
1.0, 0.1, 2000.0
0.0 0.0
5000.0 0.0 0.0          80          5      ! Profile 2
  0.0, 1536.00
  200.0, 1528.00
  700.0, 1502.00
  800.0, 1500.00
 1200.0, 1497.00
 1500.0, 1497.00
 2000.0, 1500.00
 3000.0, 1512.00
 4000.0, 1528.00
 5000.0, 1545.00
  0.
1.0, 0.1, 2000.0
0.0 0.0
4000.0 0.0 0.0          100         5      ! Profile 3
  0.0, 1536.00
  200.0, 1528.00
  700.0, 1502.00
  800.0, 1500.00
 1200.0, 1497.00
 1500.0, 1497.00
 2000.0, 1500.00
 3000.0, 1512.00
 4000.0, 1528.00
  0.
1.0, 0.1, 2000.0
0.0 0.0
5000.0, 0.0 0.0          120.         0      ! Profile 4
  0.0, 1536.00
```

Figure B6 *Input run stream for case 3.*

```
200.0, 1528.00
700.0, 1502.00
800.0, 1500.00
1200.0, 1497.00
1500.0, 1497.00
2000.0, 1500.00
3000.0, 1512.00
4000.0, 1528.00
5000.0, 1545.00
0.
1.0, 0.1, 2000.0
0.0 0.0
!LARGE
MATCH 2
NMESH 1
OPTMZ
TLRAN,COH,PLT
XAXIS 0, 200, 16, 40
YAXIS 60, 120, 10, 10
0 200 0.1
100. 300
CONDR,COH,COL
XAXIS 0, 200, 20, 40
YAXIS 0 5000 8 2500
ZAXIS 76 100 2 0
0 200 0.8
100.
```

NOTE : NMESH is set to 1 to favour execution time.
Accuracy on wavenumbers is usually very good for low order modes even when obtained as the solution from a single mesh only.
The use in this problem of the waterborne modes only favours this solution.

Figure B7 Continuation of Figure B6.

Appendix C

Summary of C-SNAP inputs

PARAMETER	EXPLANATION	UNIT	LIMIT
TITLE	Text on plots	-	≤ 80 chars
NF	Number of source frequencies	-	≤ 100
F(1) F(NF)	Source frequencies	Hz	> 0
MIN, MAX, MPROP	MIN : Lowest order mode in the source field MAX : Highest order mode in the source field MPROP : Highest order mode in the propagating field		≥ 1 ≤ 500 ≤ 500
MSP, ERMAX	MSP : Number controlling the vertical grid size required to represent the acoustic field over depth. It applies to the output options CONDR and TLDEP only. ERMAX : Accuracy criterion on wavenumbers.	km	≤ 500 ≥ 0
H0, S0, S1, RB, N2	H0 : Water depth S0 : RMS roughness of sea surface S1 : RMS roughness of sea bottom RB : Range at the beginning of the profile N2 : Controls the number of range subdivisions	m m m km	≥ 0 ≥ 0 ≥ 0 ≥ 0 < 13
Z0(1), C0(1)	Z0(1) : First sound-speed profile depth (= 0) C0(1) : First sound speed value in water	m m/s	- -
.			
Z0(M), C0(M)	Z0(M) : Last sound-speed depth (= H0) C0(M) : Last sound speed value in water	m m/s	M ≤ 100
H1, R1, B1	H1 : Thickness of sediment layer R1 : Density of sediment B1 : Compressional wave attenuation in sediment	m g/cm ³ dB/λ	≥ 0 > 0 ≥ 0
Z1(1), C1(1)	Z1(1) : First sound-speed depth (= 0) C1(1) : First sound-speed value in sediment		- -
.			
Z1(N), C1(N)	Z1(N) : Last sound-speed depth (= H1) C1(N) : Last sound-speed value in sediment	m m/s	N ≤ 100 -
R2, B2, C2	R2 : Density of subbottom B2 : Compressional wave attenuation in subbottom C2 : Compressional speed in subbottom	g/cm ³ dB/λ m/s	> 0 ≥ 0 > 0
B2S, C2S	B2S : Shear wave attenuation in subbottom C2S : Shear speed in subbottom	dB/λ m/s	(1) (2)

(1) $0 \leq B2S \leq 0.75 * B2 * (C2 / C2S) **2$

(2) $0 \leq C2S \ll C1(H1)$

⊗ : This set of parameters must be repeated for all profiles.

Figure C1 Summary of C-SNAP environmental inputs

CODE WORD	EXPLANATION
IMESH arg	By default the mode coefficients are computed with the mode amplitudes obtained on the first mesh. This is a sufficiently robust criterion for a large class of cases, as the accuracy of the mode amplitude is less sensitive to the number of mesh points than the wavenumbers are. To get maximum accuracy at the cost of increased execution time IMESH can be set as high as NMESH.
LARGE	By default, the print-out of the environmental properties, the wave number and the associated attenuation coefficients is produced for the input profiles only. The specification of this code word extends the print-out to cover every profile, including those eventually generated through interpolation ($N2 > 0$).
NMESH arg	Number of subsequent meshes used to refine the wavenumbers. To get a reasonable balance between execution time and accuracy the default choice for NMESH is 1, as in most cases the solution obtained from a single mesh is already sufficiently accurate. A good choice for higher accuracy is "NMESH 4". The ratio between the number of mesh points in any two consecutive meshes is roughly 1/3. Consequently, a ratio of 2 will exist between the first and fourth mesh.
NOCYL	The effect of cylindrical spreading is not included in the pressure field.
NOLOS	The pressure field will be obtained without any form of attenuation. The imaginary part of the wavenumber is set to 0 for all modes.
NOVOL	The effect of volume attenuation is not included in the pressure field.
NSMPL arg	In any environment, the initial number of mesh points used for solving the wave equation is automatically determined by the expression: Points_in_first_mesh= NSMPL* (Max_number_of_existing_modes) The default value for NSMPL is 8. A larger number may be required in very special cases.
OPTMZ	This code word may be used to limit the maximum number of modes which are propagated out in range. The criterion consists in removing, starting from the highest order mode, all the modes that cumulatively contribute for a minor fraction only of the total field, namely at a level corresponding to the round off error of the numerical scheme. The advantage is a speed up of the code.
PLANE	Computation will be made in plane geometry. The default choice is cylindrical geometry.
MATCH arg	1 : pressure matching at coupling interfaces. 2 : reduced-pressure matching. 3 : impedance matching (Default choice).

Figure C2 Summary of 'new default' code words

OUTPUT OPTION	EXPLANATION
CONDR	Contoured transmission loss versus depth and range
MODES	Individual mode functions versus depth
PROFL	Sound speed versus depth and range
TLDEP	Transmission loss versus depth
TLRAN	Transmission loss versus range

CALCULATION TYPE	EXPLANATION
COH	Coherent addition of modes
INC	Incoherent addition of modes

OUTPUT TYPE	EXPLANATION
COL	Colour contour plots through UNIRAS software
PLT	Plotted output (line contour plot for option CONDR)
PRT	Printed output

Figure C3 *Output options, calculations and output types*

	COH	INC	COL	PLT	PRT
CONDR	YES	YES	YES	YES	
MODES				YES	YES
PROFL				YES	
TLDEP	YES	YES		YES	YES
TLRAN	YES	YES		YES	YES

Figure C4 *Allowed combinations of code words*

CODE WORD	EXPLANATION	Unit	Default
SAXIS s1, s2, s3, s4	Sound speed axis : s1 : sound speed minimum s2 : sound speed maximum s3 : axis length s4 : tickmark spacing	m/s m/s cm m/s	1450 1650 3 25
XAXIS x1, x2, x3, x4, x5	Horizontal axis x1 : lowest data value x2 : highest data value x3 : axis length x4 : tickmark spacing x5: number of data points in smoothing window (2)	(1)	(1) 1
YAXIS y1, y2, y3, y4	Vertical axis y1 : lowest data value y2 : highest data value y3 : axis length y4 : tickmark spacing	(1)	(1)
ZAXIS z1, z2, z3, z4	Loss values z1 : minimum contour level z2 : maximum contour level z3 : level increment z4 : number of smoothings	dB dB dB -	60 110 5 0

(1) In this case units and default values are dependent on the particular output option they refer to. They are given in Figures C6a,b,c and d.

(2) Applicable to option TLRAN only.

Figure C5 *Axis identifier code words*

Input Parameter	Explanation	Unit	Default
CONDR, OP1, OP2, etc	OP1, OP2, etc... (1) : any allowed choice from Figure C4		
XAXIS x1, x2, x3, x4	Range axis x1 range minimum x2 range maximum x3 axis length x4 tickmark spacing	km km cm km	rmin rmax 16 (rmax-rmin)/5
YAXIS y1, y2, y3, y4	Depth axis y1 depth minimum y2 depth maximum y3 axis length y4 tickmark spacing	m m cm m	0 Hmax (2) 10 Hmax/5
ZAXIS z1, z2, z3, z4	Loss values z1 loss minimum z2 loss maximum z3 loss increment z4 number of smoothings	dB dB dB	60 110 5 0
rmin, rmax, delr	rmin : min range for loss calculation rmax : max range for loss calculation delr : range increment	km km km	
sd(1) sd(2) . . sd(n)	sd(1) : first source depth sd(2) : second source depth . . sd(n) : nth source depth (3)	m m m	

- (1)** At least one calculation type (COH, INC) must be specified.
- (2)** Maximum water depth from the entire environmental input.
- (3)** The maximum number of allowed source depth in a single run is 10.

Figure C6a *Contoured loss versus depth and range*

Input Parameter	Explanation	Unit	Default
MODES,OP1,OP2	OP1, OP2, (1) any allowed choice from Figure C4		
XAXIS x1, x2, x3, x4	Mode Amplitude axis		
	x1 lowest data value	(2)	-0.2
	x2 highest data value	(2)	0.2
	x3 axis length (accomodates 6 modes)	(2)	16
	x4 tickmark spacing	(2)	0.2
YAXIS y1, y2, y3, y4	Depth axis		
	y1 depth minimum	m	0
	y2 depth maximum	m	H0 (3)
	y3 axis length	cm	10
	y4 tickmark spacing	m	H0 / 5

(1) At least one output type (PLT, PRT) must be specified.

(2) $\text{SQRT}(\text{m}^2 / \text{kg})$

(3) Water depth at the origin.

NOTE : Printing and/or plotting for this option will be performed ONLY for the mode set in the source field.

Figure C6b *Individual mode functions versus depth*

Input Parameter	Explanation	Unit	Default
PROFL,PLT	The only output type is PLT		
XAXIS x1, x2, x3, x4	Range axis		
	x1 range minimum	km	0
	x2 range maximum	km	RB (1)
	x3 axis length	cm	16
YAXIS y1, y2, y3, y4	Depth axis		
	y1 depth minimum	m	0
	y2 depth maximum	m	Hmax (2)
	y3 axis length	cm	10
SAXIS s1, s2, s3, s4	Sound speed axis		
	s1 sound speed minimum	m/s	1450
	s2 sound speed maximum	m/s	1550
	s3 axis length	cm	3
	s4 ticmark spacing	m/s	20

(1) Range at the beginning of the last input sound speed profile.

(2) Maximum water depth from the entire environmental input.

Figure C6c *Sound-speed profile versus depth and range*

Input Parameter	Explanation	Unit	Default
TLDEP,OP1,OP2, etc	OP1, OP2, etc... (1) : any allowed choice from Figure C4		
XAXIS x1, x2, x3, x4	Loss axis x1 loss minimum x2 loss maximum x3 axis length x4 tickmark spacing	dB dB cm dB	60 120 16 20
YAXIS y1, y2, y3, y4	Depth axis y1 depth minimum x2 depth maximum x3 axis length x4 tickmark spacing	m m cm m	0 Hmax (2) 12 Hmax / 5
rmin, rmax, delr	rmin : minimum range for loss calculation rmax : maximum range for loss calculation delr : range increment	km km km	
sd(1) sd(2) . . sd(n)	sd(1) : first source depth sd(2) : second source depth . . sd(n) : nth source depth (3)	m m m	

(1) At least one choice for the calculation type (COH, INC) and one for the output type (PRT, PLT) must be made.

(2) Maximum water depth from the entire environmental input.

(3) The maximum number of allowed source depths in a single run is 10.

Figure C6d *Propagation loss versus depth*

Input Parameter	Explanation	Unit	Default
TLRAN, OP1, OP2, etc	OP1, OP2, etc... (1) : any allowed choice from Figure C4		
XAXIS x1, x2, x3, x4	Range axis x1 range minimum x2 range maximum x3 axis length x4 tickmark spacing	km km cm km	rmin rmax 16 (rmax-rmin)/5
YAXIS y1, y2, y3, y4	Loss axis y1 loss minimum y2 loss maximum y3 axis length y4 tickmark spacing	dB dB cm dB	50 110 10 10
rmin, rmax, delr	rmin : minimum range for loss calculation rmax : max range for loss calculation delr : range increment	km km km	
sd(1), rd(1) sd(2), rd(2) . . sd(n), rd(n)	sd(1), rd(1): 1st source/receiver depth sd(2), rd(2): 2nd source/receiver depth . . sd(n), rd(n): nth source/receiver depth (2)	m m m	

(1) At least one choice for the calculation type (COH, INC) and one for the output type (PRT, PLT) must be made.

(2) The maximum allowed number of source/receiver depths in a single run is 10.

Figure C6e *Propagation loss versus range*